Pyrolysis behaviors of organic matter (OM) with the same alkyl main chain but different functional groups in the presence of clay minerals

7 authors, including:

Peng Yuan
Chinese Academy of Sciences
163 PUBLICATIONS **5,602** CITATIONS

Dong Liu
Chinese Academy of Sciences
64 PUBLICATIONS **1,652** CITATIONS

Hongling Bu
Chinese Academy of Sciences
16 PUBLICATIONS **148** CITATIONS

Hongzhe Song
Chinese Academy of Sciences
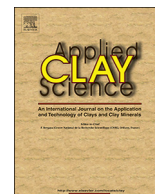**6** PUBLICATIONS **37** CITATIONS

Some of the authors of this publication are also working on these related projects:

Project   Clay Minerals View project

Project   shale gas View project

Research paper

Ethylene glycol monoethyl ether (EGME) adsorption by organic matter (OM)-clay complexes: Dependence on the OM Type

Hongling Bu[a,b], Dong Liu[a,b,*], Peng Yuan[a,b], Xiang Zhou[a,b], Hongmei Liu[a,b], Peixin Du[a,b]

[a] CAS Key Laboratory of Mineralogy, Metallogeny/Guangdong Provincial Key Laboratory of Mineral Physics and Materials, Guangzhou Institute of Geochemistry, Institutions of Earth Science, Chinese Academy of Sciences, Guangzhou 510640, China
[b] University of Chinese Academy of Sciences, Beijing 100049, China

A B S T R A C T

The ethylene glycol monoethyl ether (EGME) adsorption method has been used as an available technique for measuring the total specific surface area (TSSA) of soils and clay-rich rocks. However, the existence of organic matters (OM) has recently been proposed to affect the accurate measurement of the TSSA. To explore the effects of OM on the TSSA evaluation of clay-rich samples, EGME adsorption experiments were performed on OM and the OM-clay minerals (OM-clay) complexes that widely exist in soil and clay-rich rocks. Two types of OM, 12-aminolauric acid (ALA) and lauric acid (LA) were used, and montmorillonite (Mt) was selected as the representative clay mineral. OM-clay complexes with OM in interlayer space or OM-clay mixture with OM on the external surface of an expanding clay mineral were prepared to investigate the influence of occurrence sites of OM on the EGME adsorption. The combined methods of X-ray diffraction (XRD) and diffuse reflectance infrared Fourier transform spectroscopy (DRIFT) were used to study the structural characteristics of the OM-clay complexes before and after EGME adsorption for revealing the EGME adsorption mechanisms. The results showed both the occurrence sites and the functional groups of OM significantly influence the EGME adsorption behaviour and TSSA for OM-clay complexes. As ALA intercalated into interlayer space of Mt, it can occupy parts of adsorption sites of EGME leading to a lower TSSA than that of Mt. While as LA located on the external surface of Mt, it affects access to the interlayer surface by the EGME and occupies parts of EGME adsorption sites of the external surface of Mt, resulting in lower adsorption capability and the slight smaller TSSA than Mt. In addition, EGME reacted strongly with LA producing excess TSSA, which brings about a great difference between LA-Mt and ALA-Mt on EGME adsorption behaviour. These fundamental results demonstrated that OM could strongly affect the EGME adsorption on the OM-Mt complexes and further influence detection of TSSA. The occurrence sites and the functional groups of OM in OM-clay complex must be considered when the EGME adsorption method is used for TSSA evaluation of such clay-rich rocks and soil samples.

1. Introduction

Ethylene glycol monoethyl ether (EGME) is widely used as a polar liquid molecule probe for the determination of specific surface areas (SSA). EGME is believed to form a monolayer arrangement on the sample surface, and thus the specific surface area can be obtained based on the calculation of the number of EGME molecules and their occupied surface area (Carter et al., 1965; Cerato and Lutenegger, 2002). Different to gas adsorption methods (e.g., N_2 adsorption method to obtain BET-N_2 SSA Thommes et al., 2015), which only detect the external surface area of swelling clay minerals (e.g., Pennell et al., 1995; Yukselen and Kaya, 2006; Heister, 2014), EGME adsorption method is used to estimate the total specific surface area (TSSA, also denoted EGME SSA, is equal to the external specific surface area plus the inner specific surface area). This is because EGEM molecules can be adsorbed on the external and in interlayer surfaces of swelling clay minerals, such as montmorillonite (Mt). Therefore, EGME adsorption method is widely accepted as an effective method to measure the TSSA of clay minerals (e.g., Środoń and Macarty, 2008; Macht et al., 2011; Akin and Likos,

2014), clay-rich soils (Pennell et al., 1995; Jong, 1999; Quirk and Murray, 1999; Yukselen-Aksoy and Kaya, 2010; Pronk et al., 2013), and clay-rich rocks (e.g., Kennedy et al., 2002, 2014; Kennedy and Wagner, 2011; Derkowski and Bristow, 2012; Zhu et al., 2014, 2015; Saidian et al., 2016).

However, the accuracy of the TSSA measurement by EGME adsorption remains controversial when organic matter (OM) was present in above-mentioned natural samples (Heister, 2014). For instance, Cihacek and Bremner (1979) found that there were only slight differences in the TSSA of various soils before and after OM removal. Pronk et al. (2013) reported that there is a linear relationship between the BET-N_2 SSA and EGME SSA data found in arable soil from Ultuna, Sweden, and discovered that the linear relationship between the BET-N_2 SSA and EGME SSA was not affected by the differences in the OM content. Kennedy (2002) also demonstrated that Late Cretaceous black shale samples treated with H_2O_2 to remove OM were statistically similar to the untreated samples. On the other hand, some studies proposed that the TSSA increases with an increment of the OM content in clay-rich immature and non-altered soils (Keil et al., 1994; Mayer and

Xing, 2001). Even, OM was believed by some researchers to result in an overestimation of TSSA for soil samples, due to the change of the OM density after EGME adsorption (Chiou et al., 1993; De Jonge and Mittelmeijer-Hazeleger, 1996). Similarly, Derkowski and Bristow (2012) proposed that EGME and other polar liquids are not suitable for samples with an OM content above 3% or even lower for samples with some smectite.

One key reason for these debates is mainly attributed to uncertainty of occurrence mechanism of OM in these natural clay-rich geological samples. Actually, OM as an important component of soils and rocks coexists with clay minerals and often forms OM-clay minerals (OM-clay) complex (Theng, 1974; Theng et al., 1986; Kennedy et al., 2002; Lagaly et al., 2006; Zhu et al., 2016). Among these OM-clay complexes, OM-swelling clay minerals complexes are widely focused on because of complicacy for their structures and importance for the characteristic of soils and lithology (Theng, 1974; Zhu et al., 2016; Bu et al., 2017; Rahman et al., 2018). However, in previous studies, the attributions of OM and clay minerals in clay-rich soils and rocks were considered separately (e.g., Kennedy, 2002; Derkowski and Bristow, 2012), rather than as a whole. The unique characteristics of OM-clay based on complexation, which show great difference with the properties of the single OM or clay mineral were neglected, e.g. microstructure and hydrophility/hydrophobicity (Zhou et al., 2007), and thus result in the different EGME adsorption behaviour. Therefore, understanding the combined mechanism of OM and clay minerals in soils and clay-rich rocks and EGME adsorption behaviour of OM-clay complexes is a key to explore the influence of OM on the accuracy of the TSSA measurement.

In this work, Mt was selected as a model of the swelling clay mineral; and model organic molecules with specific functional groups, specifically, lauric acid (LA, $CH_3(CH_2)_{10}COOH$) and 12-amoniolauric acid (ALA, $NH_2(CH_2)_{11}COOH$), were used to prepare the OM-clay complexes. These two aliphatic OM have similar structures and functional groups that are usually found as important components of OM in organic-rich clay rocks or soils (Vandenbroucke and Largeau, 2007). Based on the knowledge of the intercalation chemistry of clay minerals (Lagaly et al., 2013), the amino groups of ALA is easily protonated ($-NH_3^+$) in an acidic solution; thus, it leads that ALA can be intercalated into the interlayer of Mt via cation exchange to prepare the interlayer complexes. In contrast, LA cannot intercalated into the interlayer space of the Mt because it is non-ionic. Thus, it mainly adsorbs on the external surface of Mt (Liu et al., 2018). This difference in intercalation favors the comparison of EGME adsorption behaviours on the OM-Mt interlayer complexes (OM exists inside the interlayer space) and the OM-Mt external complexes (OM appeared in the external surface of Mt). The structural characteristics of the OM-clay complexes before and after EGME adsorption were studied using X-ray diffraction (XRD) and diffuse reflectance infrared Fourier transform spectroscopy (DRIFT). EGME reacted strongly with and was retained by samples to obtain the TSSA (EGME SSA) (Carter et al., 1965; Yukselen and Kaya, 2006). Nitrogen (N_2) adsorption-desorption analysis was adopted to characterize the pore structural features of the Mt and OM-Mt complexes.

2. Materials and methods

2.1. Materials

ALA (with a purity of 98 wt%; analytical grade) and LA (with a purity of 98 wt%; analytical grade) were supplied by Tokyo Chemical Industry Co., Ltd. These chemical reagents were used without further purification. The raw Mt used for this study was from Inner Mongolia, China. Prior to the experiments, the Mt sample was purified by repeated sedimentation to remove impurities, and a < 2 μm fraction was collected and used for the experiments. According to XRD analysis, Mt sample was not detected any other minerals in the sample, except for containing minor quartz, with a purity of 97%. Before contact with the OM, Mt was modified with sodium to obtain a better swelling property
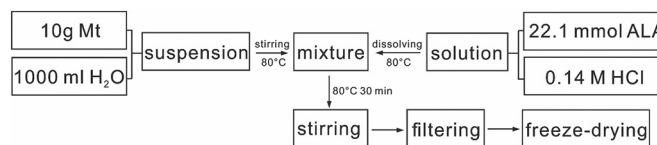

Fig. 1. The flowchart of preparation of ALA–Mt.

(hereafter labelled Mt_{Na}). The chemical composition (wt%) of the Mt_{Na} was as follows: SiO_2, 63.0%; Al_2O_3, 16.2%; Fe_2O_3, 4.9%; CaO, 0.3%; MgO, 4.6%; Na_2O, 3.6%; K_2O, 0.1%; and TiO_2, 0.4%, with a loss on ignition of 6.9%. The cation exchange capacity (CEC) of Mt was 110.50 mmol/100 g.

The preparation of the OM-Mt complex was performed according to the following procedure. For ALA, the preparation of interlayer OM-Mt complex was performed according to the following procedure. First, 22.1 mmol ALA (equal to $2.0 \times CEC$ of the Mt) was added into 200 mL of a 0.14 M HCl solution and placed in an 80 °C water bath. Then the resultant solution was added into a dispersion composed of 10 g Na–Mt and 1000 mL distilled water to form a mixture. After stirring at 80 °C for 30 min, the solid in the mixture was filtered and repeatedly washed (8 times) with large amounts of hot distilled water and then freeze-dried and ground into powder (Fig. 1) (Yuan et al., 2013; Liu et al., 2013, 2018). The product was labelled ALA–Mt. The elemental analysis shows that the content of ALA in ALA-Mt were 19.0 wt%. For LA, a simple mixing method was used to prepare the OM-Mt mixture. A total of 5 g of the Mt_{Na} sample and 1.25 g of LA were simply mixed, and the mixture was ground by ball milling for 20 min using a Pulverisette-6 planetary mill. The OM-Mt mixture was labelled LA-Mt. The content of LA in LA-Mt was 20.0 wt%. All of the above final products were passed through a 200 mesh screen for further use.

2.2. EGME adsorption tests

EGME adsorption by samples was measured by methods adopted from Eltantawy and Arnold (1973). The specific steps are as follows: approximately 1.0 g of sample was added to the weighing bottles. Before the adsorption process, the samples were dried overnight at 110 °C and allowed to remove the water molecules. EGME was added to the dry samples in each bottle. During the adsorption measurement, the samples were immersed in EGME at room temperature. The bottles were transferred to desiccators containing a mixture of dried $CaCl_2$ and EGME desiccant. And bottles were arranged around the circumference of the desiccant tray cover. The system was evacuated for 45 min under vacuum. Then the systems were allowed to stand overnight under vacuum. To prepare the desiccant, 100 g of oven-dried $CaCl_2$ was mixed with 20 mL of EGME in a culture dish, and then thoroughly stirred and put into glass dish and positioned in the base of the desiccator. Afterward, they were weighed immediately. The process of evacuation was repeated, and they were weighed until a constant weight was attained (the mass difference between the two measurements was < 0.0010 g). Three replicates each of a suite of clay mineral standards obtained from the Clay Mineral Society and included in the same batch as the samples showed good reproducibility (SAz-2: 760 m²/g ± 0.7%; SWy-2: 681 m²/g ± 0.81%). Finally, the EGME SSA (TSSA) was calculated from the equation based on the absorbed quantity of EGME molecules:

$$S_{EGME} = \Delta m/0.000286/m$$

where, S_{EGME} = TSSA, Δm = weight of the absorbed quantity of EGME (g); m = weight of dry samples (g); 0.000286 is the conversion factor, which means the weight of EGME required to form a monolayer over 1 m² surface. The resulting EGME-adsorbed samples were labelled by applying the suffix "/EGME" to the sample names. For example, Mt/EGME denotes Mt with the adsorption of EGME. In addition, a NaCl-EGME solvate (NaCl/EGME) is prepared and used for DRIFT analysis in oder to detect the EGME adsorption behaviour of Mt_{Na} since its

interlayer space is dominated by Na ions.

2.3. Characterization methods

The major element oxides were determined using a Rigaku RIX 2000 X-ray fluorescence (XRF) spectrometer on fused glass beads. Additionally, quantification of OM of the interlayer complex was determined by N elemental analysis, which was performed using an Elementar Vario EL III Universal CHNOS elemental analyzer.

X-ray diffraction (XRD) patterns of the samples were recorded on a Bruker D8 Advance diffractometer with a Ni filter and CuKα radiation (λ = 0.154 nm) using a generator voltage of 40 kV and a generator current of 40 mA with a scan rate of 1° (2θ)/min.

The DRIFT characterization was performed on the Praying Mantis™ diffuse reflection accessory (Harrick Scientific Products INC) of a Bruker Vertex-70 Fourier transform infrared spectrometer at room temperature. The spectra were collected over a range of 600–4000 cm^{-1} with 64 scans at a resolution of 4 cm^{-1}.

N$_2$ adsorption-desorption isotherms were measured with a Micromeritics ASAP2020 system at liquid-nitrogen temperature. The samples were outgassed at 110 °C for 12 h before the measurements. The specific surface areas (S_{BET}) of the samples were calculated from the nitrogen adsorption data using the multiple-point Brunauer-Emmett-Teller (BET) method (Brunauer et al., 1938).

3. Results and discussion

3.1. X-ray diffraction analysis

The XRD pattern of Mt$_{Na}$ shows a (001) diffraction reflection with a d_{001} value of 1.26 nm, which corresponds to an interlayer distance of approximately 0.30 nm because the height of a tetrahedron-octahedron-tetrahedron (TOT) layer of montmorillonite is approximately 0.96 nm (Brigatti et al., 2013). The d_{001} value for Mt$_{Na}$ after EGME adsorption is 1.48 nm, which indicating EGME has penetrated into the clay interlayers and expanded the clay by an additional 0.22 nm (see Fig. S1 in Supplementary Materials (SM)), which is close to the size of an EGME molecule (see Fig. S2 in SM). This result is consistent with previous studies demonstrating that the d_{001} value of montmorillonite increased (Eltantawy and Arnold, 1973). As reported by Kellomäki et al. (1987), compared with the initial spacing, the basal spacing d_{001} of montmorillonite increased after treatment by EGME and the increased difference is closely related to the exchangeable cation properties. These data confirm that the inner specific surface area of the Mt could be evaluated. This finding explains the previous results showing that the EGME SSA of montmorillonite is considerably higher than that of the N$_2$-BET SSA (e.g., Dogan et al., 2007; Saidian et al., 2016).

Fig. 2 shows the XRD patterns of the OM and OM-Mt complexes before and after EGME adsorption. The d_{001} value of ALA-Mt is 1.70 nm, which indicates a successful intercalation of OM into the interlayer spaces of Mt (Fig. 2a). The increase in d_{001} values represents an enlargement of the interlayer distances of Mt, which results from the replacement of the original interlayer hydrated sodium ions in Mt$_{Na}$ by the intercalated organics. The value of d_{001} for ALA-Mt corresponds to an interlayer distance of approximately 0.74 nm, indicating that the interlayer distances are greatly increased. This change occurs because the arrangement of these organics adopts a high packing-density mode, such as a tilted monolayer arrangement. Many previous studies on the intercalation chemistry of clay minerals have demonstrated that an increase in d_{001} of the OM-clay complexes is determined by the amount and the interlayer arrangement modes of the intercalated organics (Lagaly et al., 2013).

With EGME adsorption, ALA-Mt/EGME exhibits a (001) reflection with a d value of 1.83 nm (Fig. 2a), indicating the penetration of EGME into the interlayer space of Mt possibly adopted a horizontal monolayer arrangement. The data suggest that interlayer space with larger

openings favors penetration of EGME molecules, as the layer-separation energies are low. Similarity, Chiou and Rutherford (1997) compared the EGME vapors adsorption characteristics on different exchanged cation and layer charge of montmorillonite clays and found that the larger interlayer openings (entrance) favor an increase in the EGME adsorption capacity to some extent. The results suggest that the intercalation of ALA leads to much greater layer openings and changes the interlayer microstructure that ordinarily would have been available for the EGME to access. The N$_2$ adsorption-desorption isotherm of ALA-Mt indicates the decrease of the microporosity and mesoporosity and confirms the involvement of their long alkyl chains in the clay aggregation alters the porous structure (see Fig. S3 in SM). This phenomenon indicated that the expansion of the interlayer entrance of Mt resulting from the intercalated OM is the key factor for EGME penetration for OM-clay complexes in this scenario.

For LA-Mt, however, the value of d_{001} is 1.29 nm; thus, no obvious differences in the (001) reflections are observed between LA-Mt and Mt$_{Na}$ (d_{001} = 1.26 nm). The result indicates that the intercalation of the related organics did not occur as expected during the preparation, and the organics remained outside of the interlayer space of Mt. In the XRD pattern of LA-Mt/EGME, the diffraction pattern with a d value of 3.25 nm corresponds to the EGME planes, which indicates the adsorption of EGME on LA-Mt. It is noteworthy that a broadening of the (001) reflection in the case of LA-Mt/EGME (Fig. 2b) is observed. This broadening implies irregular basal spacing and therefore a low crystalline order of Mt. Furthermore, there is a significant change in the (001) reflection after EGME adsorption with a d_{001} value of 1.50 nm, indicating that a possible reason of the broadening is the very small-scale intercalation of EGME during sample adsorption. The finding means that EGME was not only adsorbed onto the external surface of Mt. for LA-Mt, but also entered into the interlayer space.

3.2. Infrared spectroscopy analysis

The DRIFT spectra of liquid EGME, NaCl/EGME, and EGME adsorbed on Mt$_{Na}$ are shown in Fig. 3. The assignments for the vibrations are summarized in Table 1, and these assignments are based on previous reports (Nguyen et al., 1987; He et al., 2004). The DRIFT spectrum of the Mt$_{Na}$/EGME exhibits vibrations that result from the combination of the characteristic bands of Mt$_{Na}$ and EGME (Fig. 3 a-b, d). As an example, these intense bands at 2978, 2937, and 2880 cm^{-1} are attributed to the asymmetric and symmetric stretches of the CH$_3$ and CH$_2$ groups. The bands in the region 1500–1100 cm^{-1} are generally due to the bending, wagging, and twisting modes of the CH$_3$ and CH$_2$ groups and the CH$_2$ of the O$_2$C$_2$H$_4$ group. These results confirm the EGME adsorption on the Mt.

However, some notable differences are described as follows. A new broad peak at 3285 cm^{-1} was noted in the spectrum of Mt$_{Na}$/EGME, which corresponds to an absorption at 3313 cm^{-1} in the spectrum of NaCl/EGME (Fig. 3c and d). This band could be assigned to the OH-stretching mode of the EGME molecule interacting directly with the Na ions. Additionally, a very weak band near 1305 cm^{-1} that appeared in the spectrum of Mt$_{Na}$/EGME is assigned to the in-plane OH-deformation mode of the adsorbed EGME coordinating to the Na ions or to the CH$_2$-wag of an EGME conformer. These results are similar to the findings of Nguyen and coworker demonstrating that the bands of the EGME molecule interacting directly with the Ca^{2+} ions occurred in the spectrum of Ca-montmorillonite with EGME adsorption (Nguyen et al., 1987). Accordingly, these observations indicate that the penetration of EGME molecules into the interlayer space of Mt$_{Na}$, which agrees with the XRD results.

The DRIFT spectra of liquid EGME, ALA and ALA-Mt before and after EGME adsorption are shown in Fig. 4. The assignments for the vibrations are summarized in Table 1, and these assignments are based on previous reports (Nguyen et al., 1987; Katti et al., 2006; Sikdar et al., 2008; Yuan et al., 2013). The DRIFT spectrum of ALA/EGME exhibits
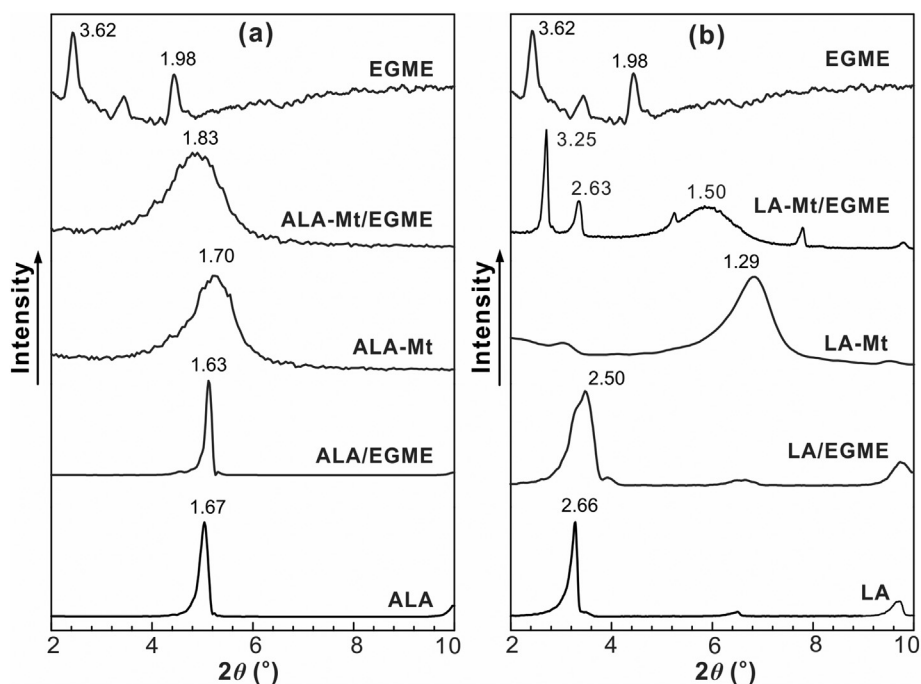
Fig. 2. X-ray diffraction patterns of samples before and after EGME adsorption. (a) ALA and ALA–Mt; (b) LA and LA-Mt.
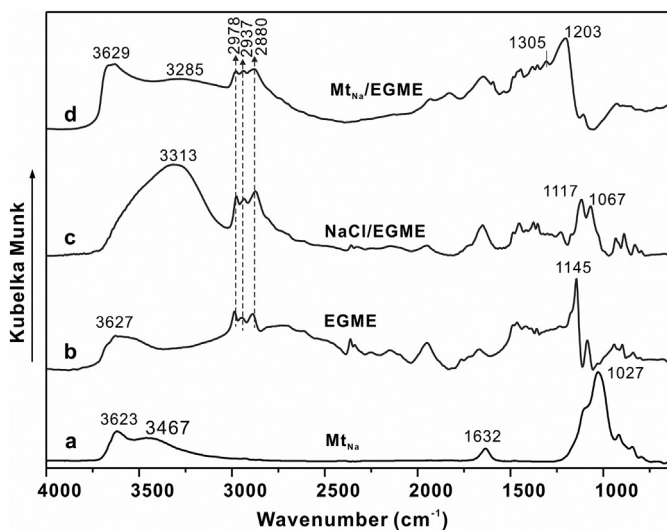

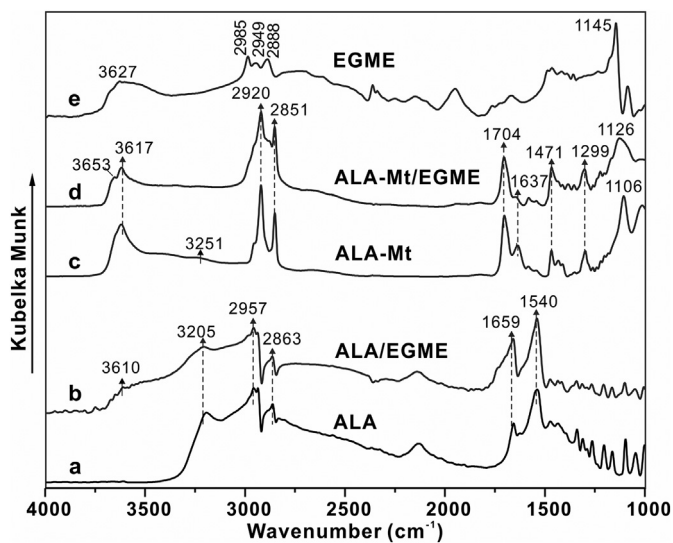**Fig. 3.** DRIFT spectra of Mt$_{Na}$, EGME, NaCl/EGME and Mt$_{Na}$/EGME.

Fig. 4. DRIFT spectra of ALA and ALA-Mt before and after EGME adsorption.

Table 1
Band assignments of the IR spectra of EGME, Mt, ALA, LA, ALA-Mt and LA-Mt before and after EGME adsorption.

Wavenumber (cm^{-1})	Band assignments	Wavenumber (cm^{-1})	Band assignments
3856/3744/3737	OH stretching	~1701/1725/1704	C=O stretching
3653/3632/3627	OH stretching H-bonded of EGME	1659	N−H bending
3623/3619/3615/3610	OH stretching of structural hydroxyl group of Mt	~1638/1637/1632	OH deformation of water
3285/3313	OH stretching interacting with Na ions	1559	C=O asymmetrical stretching
3251	NH$_3^+$ stretching	1540	Asymmetric R−COO$^-$ stretching
3205	N-H stretching	~1472	CO−H bending
3115	Olefinic CH-stretching of vinyl ethyl ether	1309/1300	Symmetric R−COO$^-$ stretching
~2956/2978	CH$_3$ asymmetrical stretching	1305	In-plane OH-deformation
~2929/2920	CH$_2$ asymmetrical stretching	1203	CH$_2$ twisting
~2880	CH$_3$ and CH$_2$ symmetrical stretching	1145/1131/1126/1117/1106/1070	C−O−C stretching
~2854/2851/2837	CH$_2$ symmetrical stretching	1027	Si-O stretching of Mt

vibrations that result from the combination of characteristic bands of ALA and EGME (Fig. 4 a and b). For instance, the bands are attributed to the characteristic bands of pure ALA, including the N−H stretching ($3205 \, cm^{-1}$), N−H bending ($1659 \, cm^{-1}$) vibration, and asymmetric R-COO^- stretching ($1540 \, cm^{-1}$) vibration (Yuan et al., 2013). The band at $2863 \, cm^{-1}$ is attributed to the combination vibration of CH_3 for EGME molecules and CH_2 for ALA. A broad band at $3610 \, cm^{-1}$ was observed, which is attributed to the OH stretching mode of the EGME molecule, as described earlier, and implies that EGME is adsorbed onto the ALA surface through physical adsorption. The other bands of ALA are generally not affected by the presence of EGME, indicating that there is no significant chemical adsorption occurs between the EGME and ALA.

For ALA-Mt, it exhibits different vibrations from those of ALA and Mt before EGME adsorption (Fig. 4 a, c). The N−H stretching vibration of -NH_2 at $3205 \, cm^{-1}$ in ALA does not appear in ALA-Mt. Instead, a weak band is observed at $3251 \, cm^{-1}$; it is assigned to the asymmetrical N−H stretching of the -NH_3^+ groups, confirming the protonation of ALA and its intercalation into the interlayer space of the Mt via cation exchange (Yuan et al., 2013). For ALA-Mt/EGME, a small shoulder band at $3653 \, cm^{-1}$ occurred, which is ascribed to the EGME units of the OH stretching vibration. The bands in the region $1500–1100 \, cm^{-1}$ were generally due to the bending, wagging, and twisting modes of the CH_3 and CH_2 groups and the methylenes of the $O_2C_2H_4$ group. Alternatively, compared with the other bands of raw ALA-Mt and EGME adsorbed ALA-Mt, there is no further significant changes of the ALA-Mt with EGME (Fig. 4d). This finding indicates that EGME adsorbs onto the surface of ALA-Mt through physical adsorption.

In addition, the band at $1637 \, cm^{-1}$ in the DRIFT spectrum of ALA-Mt is assigned to OH deformation of water in the hydration sphere within the clay interlayer. However, the intensity of this band decreases with the addition of adsorbed EGME in the DRIFT spectrum of ALA-Mt/EGME. This result shows that EGME molecules probably entered the interlayer space, which may be due to hydrogen bonding to the water molecules in the cation hydration sphere. This behaviour also explained the increase in the interlayer spacing after EGME adsorption, as described in the XRD analysis. In view that EGME adsorption behaviour analyzed by above discussion, therefore, EGME adsorption on the ALA-Mt was mainly caused by filling of accessible pores (such as interlayer pores created by intercalation of ALA) and by external surface adsorption of Mt.

The DRIFT spectra of liquid EGME, LA and LA-Mt before and after EGME adsorption are shown in Fig. 5. The assignments for the vibrations are summarized in Table 1, and these assignments are based on
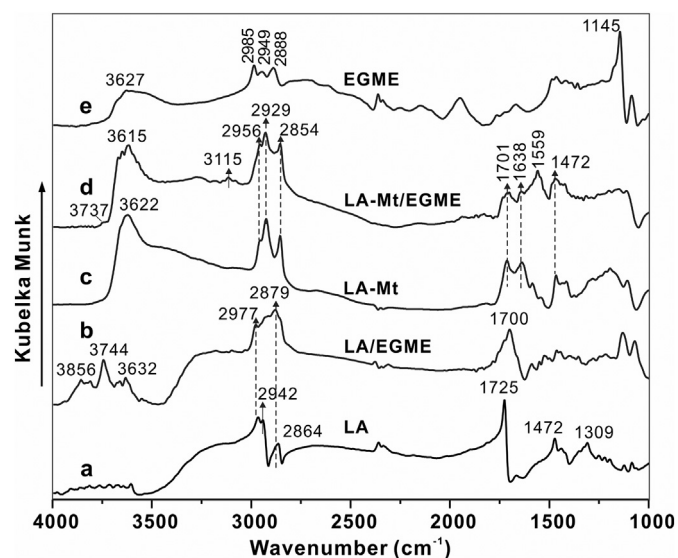
previous reports (Nguyen et al., 1987; Liu et al., 2018). For LA/EGME, the new bands at $3856 \, cm^{-1}$ and $3744 \, cm^{-1}$ tentatively attributed to the OH stretching vibration indicate hydrogen bonding between the LA and EGME molecules. In addition, a new band at $3632 \, cm^{-1}$ was noted in the spectrum that corresponded to an absorption at $3627 \, cm^{-1}$ in the spectrum of EGME (Fig. 5e), this band could be assigned to the OH stretching of the EGME. These results show that EGME has undergone a hydrogen-bond interaction with the LA molecular group.

For LA-Mt, the infrared result also shows that after the adsorption of EGME, the infrared characteristic peak of LA-Mt/EGME is the combination of LA-Mt and EGME (Fig. 5 c, d and e). However, in addition to some bands attributed to EGME and LA-Mt, a newly emerged characteristic peak at $1559 \, cm^{-1}$ is attributed to the antisymmetric stretching vibrational of C=O in LA. Therefore, the carboxyl groups in LA were affected by EGME adsorption. In addition, a new band at $3737 \, cm^{-1}$ may be attributed to the OH stretching vibration indicate of hydrogen bonding between the LA and EGME molecules. Moreover, a weaker band in the spectrum of LA-Mt at $3115 \, cm^{-1}$ was possibly assigned to traces of vinyl ethyl ether (Mikawa, 1956). The small amount of vinyl ethyl ether was probably formed by dehydration of the EGME on the clay (Nguyen et al., 1987). These results imply that a chemical reaction occurred between LA-Mt and EGME, which is mainly through a hydrogen-bond interaction with EGME with the carboxyl groups in LA. Furthermore, the intensity of the band at $1638 \, cm^{-1}$ decreases that is attributed to the OH deformation vibration of the interlayer water of Mt. This finding generally indicates that EGME may penetrate into the interlayer space of Mt. The above results show that the adsorption of EGME on LA-Mt is mainly through hydrogen-bond interactions between the external surface of LA and EGME and or onto the small pores and interlayer voids of LA-Mt.

3.3. Specific surface area analysis

From the information in Table 2, it can be seen that the EGME SSA exceeds the N_2-BET SSA (S_{BET}) in all cases. EGME shows higher uptake than N_2 for pure Mt because they can readily adsorb on siloxane surfaces and condense into small interlayer pores and voids. The EGME adsorption estimated by the above procedure is in good agreement with the above XRD and DRIFT analysis. However, for OM-Mt complexes, although the existence of OM affects the EGME adsorption behaviour (as described above) and thus adsorption capacity, where the S_{EGME} of all OM-Mt complexes exhibits more comparable values than that of S_{BET}.

In the case of ALA-Mt, there is a minimum vale in S_{EGME} and S_{BET} among the samples. It represents an extreme and instructive system, in which the layer openings before sorption are sufficiently large to permit access of a significant amount of EGME to interlayer spaces, while the EGME adsorption on the ALA-Mt is characterized by low capacities that are significantly lower than for LA-Mt and Mt_{Na}. Part of the reason why ALA-Mt exhibit less EGME capacity than expected is that the bulky ALA ion occupies a significant fraction of interlayer spaces. Moreover, this may have to do with interlayer cations solvation of the Mt on EGME adsorption. In the equilibrium state, the effect of cation on EGME uptake may follow Na > ALA. Thus, due to the Na ion was replaced by ALA ion in the interlayer space, the EGME solvation of the interlayer residual Na ion may be insignificant for ALA–Mt. As a consequence, ALA-Mt have a lower EGME adsorption capacity than Mt_{Na} and thus a lower EGME SSA than that of the Mt_{Na}. Other studies also reported relatively low EGME adsorption capacity for some interlayer OM-clay complexes (e.g., Chiou and Rutherford, 1997; Ugochukwu, 2017). For interlayer OM-Mt complexes with different contents of ALA, very slight difference of d_{001} values after EGME adsorption for various complexes (See Fig. S4 in SM) indicates that the influence of organic matter content is very little on the adsorption of EGME for ALA-Mt.

N_2 adsorption on the ALA-Mt showing the same trend compared with the Mt_{Na} and LA-Mt demonstrated a significant fraction of

Fig. 5. DRIFT spectra of LA and LA-Mt before and after EGME adsorption.

Table 2
The d_{001} values and N$_2$-BET SSA (S$_{BET}$) and EGME SSA (S$_{EGME}$) results for samples.

Sample	[a]$d_{001(before)}$ (nm)	[b]$d_{001(after)}$ (nm)	S$_{BET}$ (m²/g)	S$_{EGME}$ (m²/g)	[c]TOC (wt%)	Quantity of EGME (g/g)
Mt$_{Na}$	1.26	1.48	81.6	817.5	–	0.23
ALA-Mt	1.70	1.83	46.0	551.1	19.00	0.16
LA-Mt	1.29	1.50	11.5	705.8	20.00	0.20

[a] The d_{001} value of samples before EGME adsorption.
[b] The d_{001} value of samples after EGME adsorption.
[c] The total organic content of OM-Mt complexes.

interlayer spaces was occupied. However, EGME shows a higher uptake on ALA-Mt than that of N$_2$. In light of the interlayer distance (0.74 nm) and molecule size of N$_2$ (0.35 nm), one would expect that N$_2$ is able to enter the interlayer space of the Mt (Kaufhold et al., 2010; Michot and Villieras, 2006). The result was yet to be expected, and the fact is that the EGME capacity is much higher than the corresponding N$_2$ capacity (Table 2). This higher adsorption of EGME than N$_2$ is due primarily to EGME on ALA-Mt involves both cation solvation and lattice expansion that are not associated with N$_2$ adsorption. This may be taken as an indication that most of the EGME adoption is in pores created by the introduction of bulky ALA ions into the lattice and condense into small interlayer pores and voids.

By contrast, for LA-Mt, there is a moderate increase in EGME adsorption capacity and EGME SSA in the listed samples, but a substantial decrease in S$_{BET}$ compared with Mt$_{Na}$. A somewhat lower S$_{BET}$ for LA-Mt than that of Mt$_{Na}$ is due to that, LA existed the external surface of the Mt particles blocks the interlayer entrance, and even alters the porous structure for the involvement of their long alkyl chains in the clay aggregation, which thus is not conducive to the entry of N$_2$. However, this does not completely affect the entry of EGME (as described in XRD analysis). As noted, the EGME penetrate into the interlayer space in the case of LA-Mt. Nevertheless, the EGME SSA of LA-Mt is still slightly lower than that of Mt$_{Na}$. This effect may have to do with the OM that occurred outside of the interlayer space. For LA-Mt, EGME entered the interlayer space of Mt after long time adsorption, showing a high TSSA value; but the EGME adsorption sites on the external surface of Mt had been occupied by LA, resulting in lower adsorption capability and the slight smaller TSSA than Mt$_{Na}$. This result is in good agreement with the data of N$_2$ adsorption experiment with decrement of BET specific surface area of Mt after complexation with LA from 81.6 to 11.5 m²/g.

A comparison of the d(001) spacing of LA-Mt with different contents of LA before and after EGME adsorption provides an account of the effect of OM content on EGME adsorption. These d_{001} values of LA-Mt with different contents of LA show very little difference although the content of LA were from 1.0% to 20%, suggesting the very low relativity between LA amount and EGME amount in the interlayer space of Mt (See Fig. S5 in SM). Moreover, these larger values indicate that EGME was present in the interlayer space of Mt, showing that EGME penetrating into the interlayer space probably needs a longer time than that expected. This result also indicates the blockage of LA for EGME entrance into the interlayer space. Therefore, for the external OM-clay mixtures, EGME adsorption occurs on the external surface of OM or pores created by the introduction of LA onto the external surface, with the interlayer space of Mt playing a relatively secondary role.

Moreover, although the OM existed outside of the interlayer space affects the EGME adsorption capacity and hence the overall EGME SSA, the EGME SSA on LA-Mt exhibit more comparable values than that of ALA–Mt. The difference between the ALA-Mt and LA-Mt on EGME adsorption behaviour appears to be relatively dependent of a higher affinity to EGME molecules for the external surface LA molecules with many surface functional groups (i.e., –COOH) than pure clay minerals (i.e., Mt) with a siloxane surface or a hydroxyl surface. The organic phase of LA and LA-Mt in this study confirmed by the DRIFT absorption bands shows that carboxyl groups in LA had hydrogen-bond interaction

with EGME. The data imply that the introduction of bulky LA into the external surface plays a relatively important role in EGME adsorption, suggesting that there may be a greater affinity of EGME for the bulky LA surface of the external complex or a small degree of absorption. This trend may lead to EGME reacted strongly with and was retained by LA in the case of LA-Mt, producing excess TSSA. Thus, even though parts of inner surface area can be evaluated, these combined effects make the EGME SSA on LA-Mt higher than that ALA-Mt but lower than that of Mt$_{Na}$.

The above data indicate that the EGME SSA of OM-Mt complex was significantly affected by the nature of the OM and the association ways between OM and swelling clay minerals (i.e., inside or outside of interlayer space). The mechanism by which OM and clay were associated largely depended on the function groups of OM and they eventually determined whether or not organics could enter the interlayer space of swelling clay minerals, and results in the formation of different OM-clay complexes. The EGME adsorption on these OM-clay complexes was closely related to the microstructures. For example, the OM existed outside of the interlayer space affected the penetration of EGME to a certain extent, for the EGME adsorption sites on the external surface of Mt had been occupied by OM; moreover, even OM located into the interlayer space that may occupy the interlayer sites of EGME. Additionally, due to the different affinity between functional groups of OM and EGME molecules, these functional groups of OM play an important role in determining the EGME adsorption behaviour of OM-Mt complexes.

3.4. Implications of the effects of OM-clay complexation on EGME adsorption

The above experiments demonstrate that the effect of complexation between the organics and Mt displays different EGME adsorption behaviour. Interestingly, the interlayer space of Mt exhibits significant implications for EGME adsorption. The storage of organics in the interlayer space leads to an increase in the interlayer spacing, which in turn facilitates the penetration of EGME molecules. LA cannot enter the interlamellar domain of Mt, but its adsorption at the edge of the Mt sheet clogs the interlayer entrance pores, which is not conducive to the entry of EGME. The results indicate the importance of the organics occurring states in the interlayer space of swelling clay minerals in determining the EGME adsorption of clay-rich rocks and the EGME SSA (TSSA). These findings further imply that the surface or the microstructure of the OM-clay complexes can have a greater impact on EGME adsorption capacity and thus EGME SSA.

In reality, some studies have reported that the EGME SSA changes with the removal of OM, while other studies have reported not change. These variations have been generally ascribed to several factors including the type of clay minerals (i.e., swelling or non-swelling), the OM occurrence form (Jong, 1999) and OM components. These variations are mainly due to changes in microstructure and hydrophobicity, such as those introduced in the clay by organic cation that hinders access to the interlayer surface by EGME that is polar and hydrophilic (Ugochukwu, 2017). A deviation between BET-N$_2$ SSA and EGME SSA in the presence of swelling clay minerals and OMs has been observed in

soil samples and other sediments (Pennell et al., 1995; Yukselen and Kaya, 2006). Jong (1999) reported that the differences in the EGME SSA and internal SSA (EGME SSA-N₂ SSA) in soils reflect differences in clay mineralogy. However, when OM and clay minerals are bound together (i.e., the OM and clay mineral particles form a complex), OM will have a significant effect on the TSSA measurement. Our simulation experiments also fully illustrate this point. Consequently, attention should be paid to the accessibility of the interlayer spaces of the clays, and the possible effects of the micro-structure, and the OM occurrence state and content in mineral aggregates. The above results indicate that the swelling clay minerals and organics that coexist in the soils and clay-rich rocks may be key factors for the EGME SSA evaluation.

Moreover, the result reveals that the organics with both amino and carboxyl groups (i.e., ALA), no hydrogen-bond interaction and a physical adsorption mechanism occurs between the EGME and the organic molecules. While for the organics with carboxyl groups (i.e., LA), it was found carboxyl groups in LA had hydrogen-bond interaction with EGME. The presence of amino groups seems to affect the chemical bonding for carboxyl groups for the organics and alcohol groups for the EGME, thus, the amino group (-NH₂) of OM is responsible for the chemical adsorption between OM-clay complexes and EGME molecules. The present observation seems to indicate that EGME adsorption capacity and EGME SSA are generally related with the functional groups of OM for evaluating the TSSA of clay-rich rocks samples. In light of this consequence, analysing the properties of OM is recommended as a more suitable pretreatment for TSSA measurements in OM-rich clay rocks.

It is noteworthy that, according to previous reports, the natural OM-clay complexes normally exhibit diverse EGME adsorption behaviour, because of the high complexity of the types of organics in natural sediments. For instance, previous studies have shown that the nature of the OM causes swelling of the polymeric matrix and subsequent alteration of the micropore structure if the EGME molecules penetrate into the organic material, resulting in unreasonably high EGME SSA values (e.g., Chiou et al., 1993; De Jonge and Mittelmeijer-Hazeleger, 1996). However, it seems that the extent of this reaction depends on the nature of the OMs. In a study on organic-rich rocks with a varying degree maturity, the less mature kerogen exhibited a stronger dissolution effect by EGME than the more mature kerogen (Derkowski and Bristow, 2012). Therefore, the above facts indicate that the situation for natural OM-clay complexes is more complicated than the simulation in this study, in which sole and pure organics were used. Even so, the fundamental correlations between OM-clay complexation and the structures of the complexes revealed by this work will constitute a base for identifying natural OM-clay complexes as well as evaluating the properties of the OM-clay complexes in given samples. In future work, it would be very meaningful to analyse the content of OM, type of OM (i.e., functional groups) and association between OM and clays in clay-rich rocks from different sources (e.g., varying thermal maturities). It is worth mentioning that, the EGME adsorption method for evaluating the TSSA of clay-rich rocks with many swelling clays and soluble organics requires careful uses, especially for immature or low-maturity clay-rich rocks with a considerable amount of swelling clays.

4. Conclusions

In this work, EGME adsorption behaviour of OM with different functional groups occurring inside and outside of the Mt interlayer was studied. Different effects of OM on EGME adsorption behaviour were observed in different types of OM-Mt complexes. The functional groups and occurrence sites of OM significantly influence the EGME adsorption behaviour and EGME SSA for OM-Mt complexes. The result is due to the microstructure of OM-Mt complexes and nature of OM. ALA in the interlayer of Mt resulting in layer openings before sorption is sufficiently large to permit access of a significant amount of EGME to interlayer spaces. However, the presence of ALA in interlayer space of Mt occupied parts of adsorption sites of EGME, thus, the obtained TSSA is smaller than that of Mt. LA presents on the external surface of Mt occupied parts of EGME adsorption sites on the external surface of Mt, resulting in lower adsorption capability and the slight smaller TSSA than Mt. In addition, the functional groups of OM are found to have significantly influence on the EGME adsorption. Carboxyl groups in LA had hydrogen-bond interaction with EGME, thus lead to EGME reacted strongly with LA producing excess TSSA; while, although ALA simultaneously possesses both amino and carboxyl groups, no hydrogen-bond interaction was present and only physical adsorption occurred between the EGME and ALA. The findings of this work demonstrated that the coexistence of swelling clay minerals and OMs strongly affect the EGME adsorption behaviour and EGME SSA. Thus, it can be inferred that the EGME SSA (TSSA) of clay-rich rocks may depend on the nature of the OM, and its association with clay minerals (i.e., inside or outside of the interlayer). These issues shoud be considered in a future work when the EGME adsorption method is used to evaluate the TSSA of soils or clay-rich rocks.

Appendix A. Supplementary data

Supplementary data to this article can be found online at https://doi.org/10.1016/j.clay.2018.11.026.

References

Akin, I.D., Likos, W.J., 2014. Specific surface area of clay using water vapor and EGME sorption methods. Geotech. Test. J. 37 (6), 20140064.

Brigatti, M.F., Galan, E., Theng, B.K.G., 2013. Structure and mineralogy of clay minerals. In: Bergaya, F., Lagaly, G. (Eds.), Handbook of Clay Science: Developments in Clay Science. vol. 5. Elsevier, pp. 21–81.

Brunauer, S., Emmett, P.H., Teller, E., 1938. Adsorption of gases in multimolecular layers. J. Am. Chem. Soc. 60 (2), 309–319.

Bu, H., Yuan, P., Liu, H., Liu, D., Liu, J., He, H., Zhou, J., Song, H., Li, Z., 2017. Effects of complexation between organic matter (OM) and clay mineral on OM pyrolysis. Geochim. Cosmochim. Acta 212, 1–15.

Carter, D.L., Heilman, M.D., Gonzalez, C.L., 1965. Ethylene glycol monoethyl ether for determining surface area of silicate minerals. Soil Sci. 100 (5), 356–360.

Cerato, A.B., Lutenegger, A.J., 2002. Determination of surface area of fine-grained soils by the Ethylene Glycol Monoethyl Ether (EGME) Method. Geotech. Test. J. 25 (3), 315–321.

Chiou, C.T., Rutherford, D.W., 1997. Effects of exchanged cation and layer charge on the sorption of water and EGME vapors on montmorillonite clays. Clay Clay Miner. 45 (6), 867–880.

Chiou, C.T., Rutherford, D.W., Manes, M., 1993. Sorption of N₂ and EGME vapors on some soils, clays, and mineral oxides and determination of sample surface areas by use of sorption data. Environ. Sci. Technol. 27 (8), 1587–1594.

Cihacek, L.J., Bremner, J.M., 1979. A simplified ethylene glycol monoethyl ether procedure for assessment of soil surface area. Soil Sci. Soc. Am. J. 43 (4), 821–822.

De Jonge, H., Mittelmeijer-Hazeleger, M.C., 1996. Adsorption of CO2 and N2 on soil organic matter: nature of porosity, surface area, and diffusion mechanism. Environ. Sci. Technol. 30 (12), 408–413.

Derkowski, A., Bristow, T.F., 2012. On the problems of total specific surface area and cation exchange capacity measurements in organic-rich sedimentary rocks. Clay Clay Miner. 60 (4), 348–362.

Dogan, M., Dogan, A.U., Yesilyurt, F.I., Alaygut, D., Buckner, I., Wurster, D.E., 2007. Baseline studies of the clay minerals society special clays: specific surface area by the Brunauer Emmett Teller (BET) method. Clay Clay Miner. 54 (1), 62–66.

Eltantawy, I.M., Arnold, P.W., 1973. Reappraisal of ethylene glycol mono-ethyl enther (EGME)method for surface area estimations of clays. Eur. J. Soil Sci. 24 (2), 232–238.

He, H., Frost, R.L., Zhu, J., 2004. Infrared study of HDTMA+ intercalated montmorillonite. Spectrochim. Acta A Mol. Biomol. Spectrosc. 60 (12), 2853–2859.

Heister, K., 2014. The measurement of the specific surface area of soils by gas and polar

liquid adsorption methods—Limitations and potentials. Geoderma 216, 75–87.

Jong, E.D., 1999. Comparison of three methods of measuring surface area of soils. Can. J. Soil Sci. 79 (2), 345–351.

Katti, K.S., Sikdar, D., Katti, D.R., Ghosh, P., Verma, D., 2006. Molecular interactions in intercalated organically modified clay and clay-polycaprolactam nanocomposites: experiments and modeling. Polymer 47 (1), 403–414.

Kaufhold, S., Dohrmann, R., Klinkenberg, M., Siegesmund, S., Ufer, K., 2010. N$_2$-BET specific surface area of bentonites. J. Colloid Interface Sci. 349 (1), 275–282.

Keil, R.G., Montlucon, D.B., Prahli, F.G., 1994. Sorption preservation of labile organic matter in marine sediments. Nature 370 (6490), 549–551.

Kellomäki, A., Nieminen, P., Ritamäki, L., 1987. Sorption of ethylene glycol monoethyl ether (EGME) on homoionic montmorillonites. Clay Miner. 22 (3), 297–303.

Kennedy, M.J., Wagner, T., 2011. Clay mineral continental amplifier for marine carbon sequestration in a greenhouse ocean. Proc. Natl. Acad. Sci. U. S. A. 108 (24), 9776–9781.

Kennedy, M.J., Pevear, D.R., Hill, R.J., 2002. Mineral surface control of organic carbon in black shale. Science 295 (5555), 657–660.

Kennedy, M.J., Löhr, S.C., Fraser, S.A., Baruch, E.T., 2014. Direct evidence for organic carbon preservation as clay-organic nanocomposites in a Devonian black shale; from deposition to diagenesis. Earth Planet. Sci. Lett. 388 (18), 59–70.

Lagaly, G., Ogawa, M., Dékány, I., 2006. Clay minerals organic interactions. In: Bergaya, F., Theng, B.K.G., Lagaly, G. (Eds.), Handbook of Clay Science: Developments in Clay Science. vol. 1. Elsevier, Amsterdam, pp. 309–358.

Lagaly, G., Ogawa, M., Dékány, I., 2013. Clay mineral-organic interactions. In: Bergaya, F., Lagaly, G. (Eds.), Handbook of Clay Science: Developments in Clay Science. Vol. 5. Elsevier, Amsterdam, pp. 435–505.

Liu, H., Yuan, P., Qin, Z., Liu, D., Tan, D., Zhu, J., He, H., 2013. Thermal degradation of organic matter in the interlayer clay–organic complex: a TG-FTIR study on a montmorillonite/12-aminolauric acid system. Appl. Clay Sci. 81, 398–406.

Liu, H., Yuan, P., Liu, D., Bu, H., Song, H., Qin, Z., He, H., 2018. Pyrolysis behaviors of organic matter (OM) with the same alkyl main chain but different functional groups in the presence of clay minerals. Appl. Clay Sci. 153, 205–216.

Macht, F., Eusterhues, K., Pronk, G.J., Totsche, K.U., 2011. Specific surface area of clay minerals: comparison between atomic force microscopy measurements and bulk-gas (N$_2$) and -liquid (EGME) adsorption methods. Appl. Clay Sci. 53, 20–26.

Mayer, L.M., Xing, B., 2001. Organic matter–surface area relationships in acid soils. Soil Sci. Soc. Am. J. 65, 250–258.

Michot, L.J., Villieras, F., 2006. Surface area and porosity. In: Bergaya, F., Theng, B.K.G., Lagaly, G. (Eds.), Handbook of Clay Science. Handbook of Clay Science: Developments in Clay Science. vol. 1. Elsevier, Amsterdam, pp. 965–972.

Mikawa, Y., 1956. Characteristic absorption bands of vinyl ethers. Bull. Chem. Soc. Jpn. 29, 110–115.

Nguyen, T.T., Raupach, M., Janik, L.J., 1987. Fourier-transform infrared study of ethylene glycol monoethyl ether adsorbed on montmorillonite implications for surface area measurements of clays. Clay Clay Miner. 35 (1), 60–67.

Pennell, K.D., Abriola, L.M., Boyd, S.A., 1995. Surface area of soil organic matter reexamined. Soil Sci. Soc. Am. J. 59 (4), 1012–1018.

Pronk, G.J., Heister, K., Woche, S.K., Totsche, K.U., Kögel-Knabner, I., 2013. The

phenanthrene-sorptive interface of an arable topsoil and its particle size fractions. Eur. J. Soil Sci. 64 (1), 121–130.

Quirk, J.P., Murray, R.S., 1999. Appraisal of the Ethylene Glycol Monoethyl Ether Method for measuring hydratable surface area of clays and soils. Soil Sci. Soc. Am. J. 63 (4), 839–849.

Rahman, H.M., Kennedy, M., Löhr, S., Dewhurst, D.N., Sherwood, N., Yang, S., Horsfield, B., 2018. The influence of shale depositional fabric on the kinetics of hydrocarbon generation through control of mineral surface contact area on clay catalysis. Geochim. Cosmochim. Acta 220, 429–448.

Saidian, M., Godinez, L.J., Prasad, M., 2016. Effect of clay and organic matter on nitrogen adsorption specific surface area and cation exchange capacity in shales (mudrocks). J. Nat. Gas Sci. Eng. 33, 1095–1106.

Sikdar, D., Katti, K.S., Katti, D.R., 2008. Molecular interactions alter clay and polymer structure in polymer clay nanocomposites. J. Nanosci. Nanotechnol. 8 (4), 1638–1657.

Środoń, J., Macarty, D.K., 2008. Surface area and layer charge of smectite from CEC and EGME/H2O-retention measurements. Clay Clay Miner. 56 (2), 155–174.

Theng, B.K.G., 1974. The Chemistry of Clay–Organic Reactions. John Wiley & Sons Inc, New York.

Theng, B.K.G., Churchman, G.J., Newman, R.H., 1986. The occurrence of interlayer clay–organic complexes in two New Zealand soils. Soil Sci. 142 (5), 262–266.

Thommes, M., Kaneko, K., Neimark, A.V., Olivier, J.P., Rodriguez-Reinoso, F., Rouquerol, J., Sing, K.S.W., 2015. Physisorption of gases, with special reference to the evaluation of surface area and pore size distribution (IUPAC Technical Report). Pure Appl. Chem. 87 (9-10), 1051–1069.

Ugochukwu, U.C., 2017. Measurement of surface area of modified clays by ethylene glycol monoethyl ether method. Asian J. Chem. 29 (9), 1891–1896.

Vandenbroucke, M., Largeau, C., 2007. Kerogen origin, evolution and structure. Org. Geochem. 38 (5), 719–833.

Yuan, P., Liu, H., Liu, D., Tan, D., Yan, W., He, H., 2013. Role of the interlayer space of montmorillonite in hydrocarbon generation: an experimental study based on high temperature–pressure pyrolysis. Appl. Clay Sci. 75-76, 82–91.

Yukselen, Y., Kaya, A., 2006. Comparison of methods for determining specific surface area of soils. J. Geotech. Geoenviron. 132 (7), 931–936.

Yukselen-Aksoy, Y., Kaya, A., 2010. Method dependency of relationships between specific surface area and soil physicochemical properties. Appl. Clay Sci. 50, 182–190.

Zhou, Q., Frost, R.L., He, H., Xi, Y., Liu, H., 2007. Adsorbed para-nitrophenol on HDTMAB organoclay—a TEM and infrared spectroscopic study. J. Colloid Interface Sci. 307 (2), 357–363.

Zhu, X., Cai, J., Wang, X., Zhang, J., Xu, J., 2014. Effects of organic components on the relationships between specific surface areas and organic matter in mudrocks. Int. J. Coal Geol. 133, 24–34.

Zhu, X., Cai, J., Song, G., Ji, J., 2015. Factors influencing the specific surface areas of argillaceous source rocks. Appl. Clay Sci. 109-110, 83–94.

Zhu, X., Cai, J., Liu, W., Lu, X., 2016. Occurrence of stable and mobile organic matter in the clay-sized fraction of shale: significance for petroleum geology and carbon cycle. Int. J. Coal Geol. 160–161, 1–10.